Research Article

Improvement of Sheet Metal Properties by Inducing Residual Stresses into Sheet Metal Components by Embossing and Reforming

Stefan Walzer* and Mathias Liewald
Institute for Metal Forming Technology (IFU), University of Stuttgart, Stuttgart, Germany

Nicola Simon and Jens Gibmeier
Institute for Applied Materials (IAM–WK), Karlsruhe Institute of Technology (KIT), Karlsruhe, Germany

Hannes Erdle and Thomas Böhlke
Institute of Engineering Mechanics, (ITM), Karlsruhe Institute of Technology (KIT), Karlsruhe, Germany

* Corresponding author. E-mail: Stefan.Walzer@ifu.uni-stuttgart.de DOI: 10.14416/j.asep.2021.09.006
Received: 10 February 2021; Revised: 7 April 2021; Accepted: 18 June 2021; Published online: 13 September 2021

Abstract
In sheet metal forming, combination of embossing and reforming allows the mechanical properties of sheet metal materials to be specifically improved. Here, local property modification is achieved by the residual stresses induced as a result of the one-sided embossing process followed by a reforming step. The residual stresses induced in this specific way can lead to a significantly increase in the fatigue strength of processed sheet metal components. However, in order to ensure this kind of component optimization in continuous operation, the induced stresses have to be homogeneous. In this respect, the main objective of the study reported about in this paper was to identify a forming strategy, consisting of the process steps embossing and reforming, that generates preferably homogeneous residual stress distributions into sheet metal blanks. For this, numerical and experimental investigations were carried out with samples of the stainless steel (X6Cr17) having a thickness of 1.5 mm. It was found that embossing and reforming, integrated into a conventional forming process, is a novel approach to specifically induce very localized homogeneous compressive residual stresses in sheet metal materials. This eliminates the need for costly post-processing by means of surface treatment.

Keywords: Residual stresses, Sheet metal material, Embossing, Reforming

1 Introduction

In recent years, both industry and institutional research have been endeavoring to reduce weight and thus material demand of sheet metal products, aiming to save energy and resources on the one hand and to meet increasing lightweight challenges on the other hand. As a consequence, a huge amount of sheet metal materials commonly used in automotive engineering today are being replaced by high strength steel materials having comparatively low sheet thicknesses [1]. However, a reduction in sheet metal thickness can also lead to a reduction in fatigue strength and stiffness of the sheet metal components [2]. In this context, one common approach for extending the fatigue life of technical components is a post-processing mechanical surface treatment such as shot peening or deep rolling. Such mechanical surface treatments are intentionally applied and have been found to induce compressive residual stresses (RS) into the surface layer of the components,

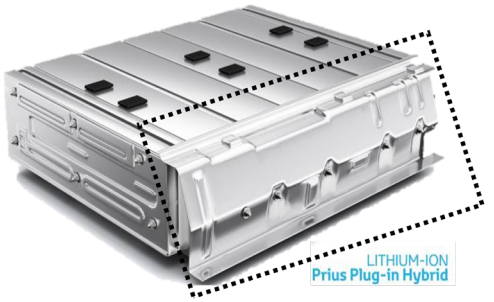

Figure 1: Sheet metal profile, which adapts the lithium-ion accumulator to the e-mobile frame [6].

which in most cases counteract the tensile loads applied externally during service and thus beneficially affect component´s fatigue performance [3], [4]. Regarding sheet metal components, local embossing also offers an alternative approach for targeted local induction of beneficial RS. The embossing structure can be considered, for example, in the shape of the deep drawing punch or die geometry, thus enabling an integrated manufacturing process in which local RS can be selectively induced during sheet metal forming. As a consequence, the application of cost and time-consuming post-surface treatments can be omitted.

Sheet metal profiles as shown in Figure 1 are used in many technical applications to absorb forces and torques [5]. In electro-driven vehicles, for example, such profiles serve to carry and secure heavy battery packs. Thereby, the profiles are constantly exposed to superimposed static and dynamic loads, which may lead to failure due to material fatigue of these types of sheet metal components.

The objective of the problem described above is to locally emboss and reform the components and thus induce homogeneous compressive RS into the areas that are predominantly subjected to tensile loading stresses during operation. The induced compressive RS counteract the tensile stresses and thus delay premature failure of the component [7]. In this respect, finite-element (FE) simulations of an embossed and subsequently reformed sheet metal bending angle specimen were carried out to identify a suitable strategy.

In order to describe and analyze the static and dynamic-mechanical load capacity of sheet metal profiles, a mechanical-static FEM-analysis was carried out with a load-compliant demonstrator specimen as designed in Figure 2. The demonstrator has a total

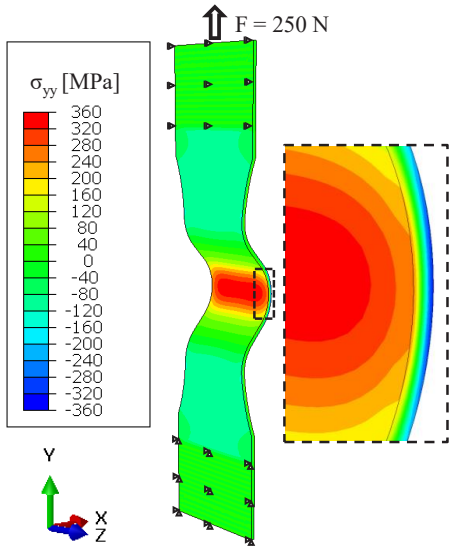

Figure 2: Sheet metal specimen for static- and dynamic fatigue analyses under tension - swell loading.

length of 170 mm and a lug width of 40 mm. The failure-critical radius is R 15 on the inside. The height from the inside of the radius to the clamping lugs is 30 mm.

The specimens are fixed on one side and loaded to a tensile force of approx. 250 N on the other side, in this case. The 250 N corresponds to a load approx. 20% below the yield strength in the cross-section of the sheet metal specimen. This ensures that the specimen is loaded just in the elastic range but is not plastically deformed. In the failure-critical radius area, tensile stresses of up to 360 MPa are located at the inside and compressive stresses of up to –360 MPa on the outside of the radius, as shown in Figure 2.

2 Embossing and Reforming Method

The manufacturing process of local embossing and reforming is divided into two process steps and should be considered separately within two operations even when combined with a conventional forming process, such as crash forming or deep drawing. The first embossing operation consists of a near-surface structuring process of the sheet metal blank, as depicted in Figure 3. Here, a structured embossing punch is used to locally plastically deform the material close to the surface, thus inducing RS into the sheet metal blank.

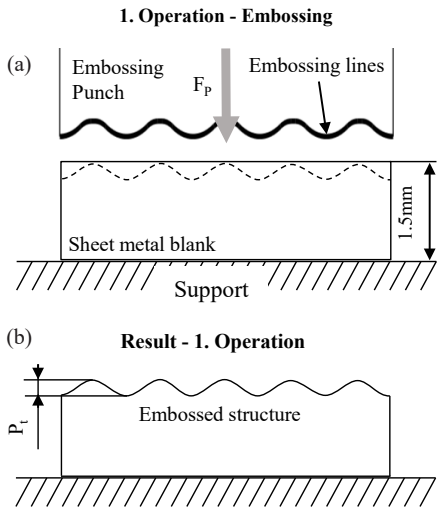

Figure 3: First operation – (a) embossing of embossign & reforming method, (b) structure after embossing.

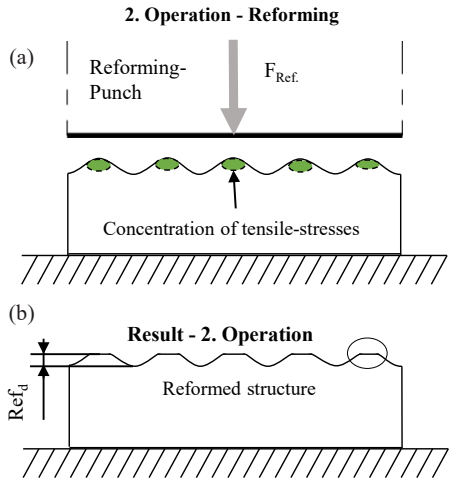

Figure 4: Second operation – (a) reforming of embossign & reforming method, (b) structure after reforming.

Initial investigations have already shown that this embossing process induces compressive RS, especially in the dimples of the produced structures. However, as a stress equilibrium is set up in a closed mechanical system, it can be expected that these embossing induced compressive RS are compensated by tensile RS in the vicinity of the embossed structure (Figure 4). Since these concentrations of tensile RS counteract the aspired homogeneous induction of compressive RS, the peaks of the structure are leveled again in an additional process step, referred to as reforming (Figure 4). By reforming the peaks, the material is plasticized and compressed again, thus relieving the tensile RS and homogenizing the compressive RS.

3 Material

For the numerical and experimental investigations on the sequential embossing and reforming process reported about in this paper, ferritic stainless steel sheets X6Cr17 with a thickness of 1.5 mm were used. The materials chemical composition is given in Table 1. The single-phase stainless steel was chosen in fact that the battery boxes should be protected against corrosive environmental conditions. Furthermore, the X6Cr17 with a relatively low yield strength and tensile strength has the similar good forming capacity as classic deep drawing steels as e.g. HC360L.

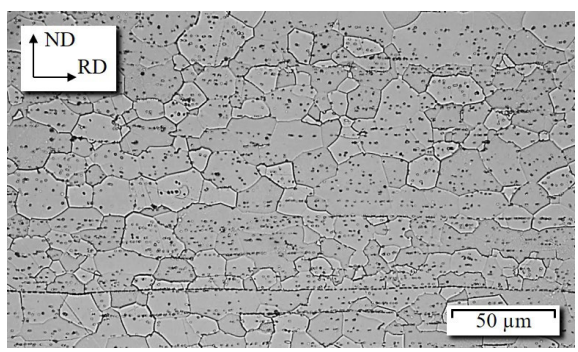

Figure 5: microstructure of the cold-rolled sheet metal X6Cr17 (rolling direction horizontal).

Table 1: Chemical composition of X6Cr17 in wt. %

C	Si	Mn	Cr	Ni	Cu	Fe
0.034	0.38	0.35	16.07	0.24	0.21	bal.

In Figure 5, a micrograph of the as-received state of the sheet metal blanks is shown. The cross-sectional view depicts the ferrite grains with an average size of approx. 20 µm and linear-shaped carbide arrays along the rolling direction (RD).

The materials crystallographic texture was analyzed using X-ray diffraction. A diffractometer of type Seifert XRD 3003 PTS with iron-filtered Co-Kα radiation was used with a 1 mm pin hole collimator as primary aperture and a 4 mm slit on the secondary

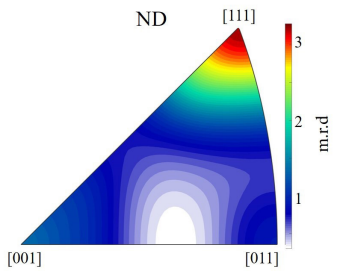

Figure 6: crystallographic texture given by the inverse pole figure in normal direction (ND).

side in front of the scintillation counter. From the four measured pole figures {100}, {200}, {211} and {220}, the orientation distribution function (ODF) was calculated and the inverse pole figure (IPF) was obtained (Figure 6). The IPF indicates that in the initial state the X6Cr17 sheets show a weakly pronounced typical rolling texture for bcc metals.

Tensile tests have been performed for rolling direction, 45° direction, and transverse direction. The mechanical properties determined this way are given in Table 2. From texture analysis and tensile tests, it is concluded that the cold-rolled material possesses weakly pronounced anisotropic mechanical properties.

Table 2: Mechanical properties of X6Cr17

Direction	E-Modul [GPa]	$Rp_{0.2}$ [MPa]	Rm [MPa]	Ag [%]	A_{80} [%]	r [-]	n [-]
0°	212	354	487	17,1	32,4	0,72	0,18
45°	215	374	503	16,9	26,3	0,79	0,17
90°	213	378	510	15,7	27,5	0,81	0,17

4 Numerical Method

The aim of the numerical investigations was to analyse and establish the process of embossing & reforming as a novel method to induce homogeneous compressive RS in the sheet metal surface. Furthermore, to induce RS distributions in the sheet metal, which are homogeneous to the greatest possible extent by making specific changes to the embossing punch geometries in order to optimize the tool accordingly.

4.1 *FE - modeling*

The numerical simulation of the sequential embossing and reforming process was performed by means of finite element modeling. The model surfaces and the tool were designed in CATIA and subsequently imported into the commercial FE-software STAMPACK V7.2.2 (Figure 7). For the simulations, an element number of 5 over the blank thickness of s_0 = 1.5 mm was chosen. The simulation model was set up with hexahedral fully integrated solid elements with size of 0.2 mm × 0.2 mm and a height of 0.3 mm to discretize the blank. In contrast, rigid shell elements were used to discretize the tools. No mass scaling was used in the simulations. The anisotropic behavior of the material was taken into account by implementing the Lankford coefficients (r – values) determined from the tensile tests performed in three different sheet metal orientations according to the Hill yield criterion [8]. Contact modeling between the blank and tool surfaces was implemented using Coulomb friction and a friction coefficient of $\mu = 0.12$. The explicit dynamic algorithm was used to emboss and reform the blanks and the implicit algorithm to simulate the spring back, respectively. Especially for the calculation of stress and strain conditions occurring during the process and after springback, flow curves had to be specified up to the maximum strain. The macroscopic flow resistance of the sheet metal material was modeled using a stress strain model that was analytically approximated according to the Ludwik-Hollomon extrapolation method [9]. The material parameters used in the model were as follows: Young's modulus of 213 GPa, Poisson's ratio of 0.33, mass density of 7.850 kg/m^3, yield stress of 369 MPa, and tensile stress of 500 MPa.

Figure 7 shows the process principle of the sequential embossing and reforming process of the sheet metal bending angle specimen. As explained in the process description, forming of the component takes place within the 1st operation (Figure 7, left). The embossing punch is forming the sheet angle specimen into the forming die. When the lower dead center is reached, the embossing lines [Figure 8(b)] are imprinted into the sheet angle specimen´s surface. In a second operation the created structure is reformed of around 0.020 mm with a flat reforming punch (Figure 7, right).

4.2 *Study to identify suitable embossing geometry*

In order to define the best possible punch-geometries for the forming operations, a numerical variant study

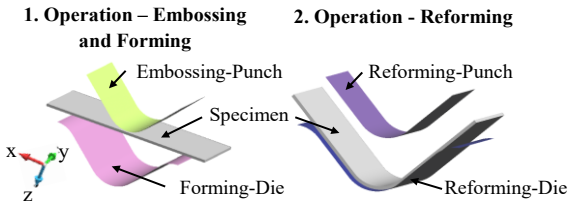

Figure 7: numerical model of the embossing and reforming process to manufacture the sheet bending angle specimen; 1. Operation embossing and forming (left), 2. Operation – reforming (right).

with differently defined geometries was carried out (Table 3). For this purpose, the number of embossing lines and the distances between them were varied. The radii of the embossing lines and the radii of the dimples were also changed in several iteration steps in order to identify those punch geometries with the most homogeneous stress distributions over the section cut A-A (Figure 8). Based on these criteria, a simulation study was conducted and the results are presented below using two selected punch configurations.

In order to avoid possible damage to the sheet metal and stress peaks caused by sharp edges, comparatively soft contours with different radii were used in these studies. For these reasons, the punch configuration 14 × 2.0 [Figure 8(b)] was modeled as a first approach, which has 14 parallel embossing lines next to each other. The radius of the semicircular embossing lines is 2 mm and the distance between the individual embossing lines is 1.8 mm. The geometry allows a maximum embossing depth of 0.1 mm. Starting from this first approach different variants were studied by applying a systematic variation in the number of embossing lines, the peak radii, the ground radii, and the distance between the embossing lines. In comparison to the first approach of the punch geometry (14 × 2.0) the variant that gave the supposedly best result regarding our desired objectives is listed in Table 3 (26 × 0.5).

Table 3: Punch configurations used for numerical investigations

	Punch_config 14 × 2.0	**Punch_config 26 × 0.5**
No. of Embossing-lines	14	26
Peak radius	2.0 mm	0.5 mm
Ground radius	2.0 mm	0.5 mm
Distance between embossing lines	1.8 mm	0.6 mm

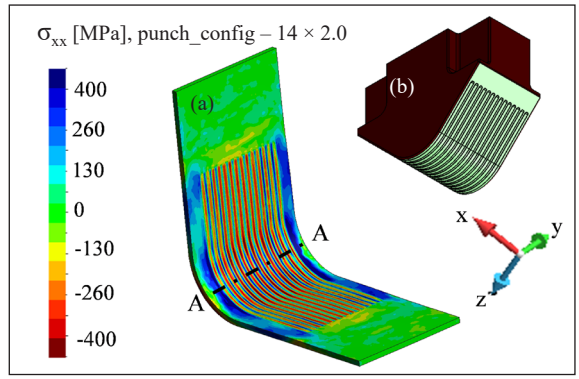

Figure 8: σ_{xx} residual stresses of sheet metal bending angle specimen in x-direction (a) of punch configuration 14 × 2.0 (b).

4.3 *Residual stress distribution after embossing*

Initial simulations with the different punch configurations have shown that large-area embossing structures require extremely high forces up to about 800 kN for the embossing step on the one hand and to deform the sheet angle specimen globally in width and length on the other hand. This counteracts the development of homogeneous RS in the upper surface layer of the components. Furthermore, it was observed that the larger the deformations in width and length of the sheet angle specimen, the lower the resulting RS within the embossed area are.

Regarding the stress distribution on the surface of the section cut A-A in Figure 8(a), it is obvious that punch configuration 14 × 2.0 creates both compressive and tensile RS. In this respect, the calculated RS distribution shows a periodic sinusoidal characteristic along the embossed structure (Figure 9). Here, it can be noticed that very homogeneous compressive residual stresses of up to 305 MPa occur in the embossed areas (dimples). In the unembossed areas (bulges) located between these dimples, the generated compressive RS are balanced by tensile RS up to an approximately equal magnitude of about 320 MPa. These bulges still exhibit the initial sheet thickness of 1.5 mm, i.e. they were not subjected to any plastic deformation induced by the embossing process.

The simulation results shown in Figure 9 indicate that the punch configuration 14 × 2.0 did not achieve the desired aim of inducing sufficiently homogeneous compressive RS into the sheet metal surface. For this

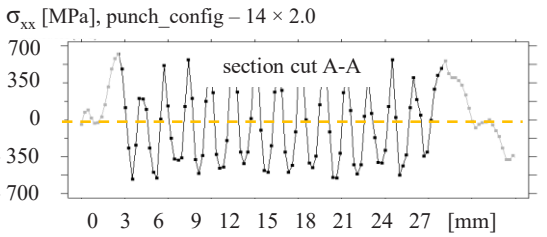

Figure 9: Residual stresses σ_{xx} of sheet metal bending specimen after embossing along section cut A-A (topside).

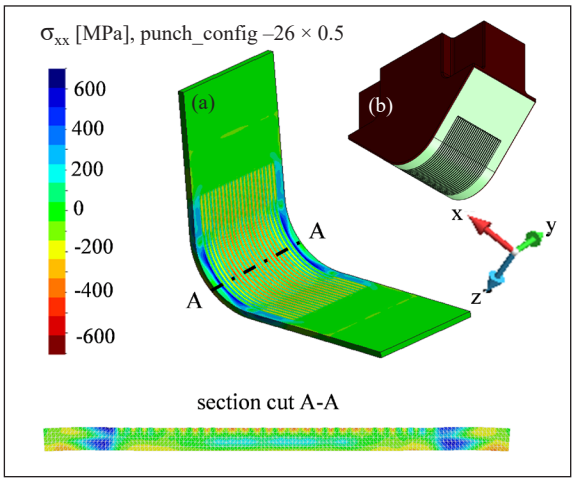

Figure 10: residual stresses σ_{xx} of sheet metal bending angle specimen in x-direction (a) of punch configuration 26 × 0.5 (b)

purpose, the punch geometry was modified in a further simulation study such that the radii of the embossing lines were significantly reduced on the one hand and the number of individual embossing lines was increased on the other hand. By the higher number of embossing lines, it was intended to keep the distance between the dimple areas as small as possible in order to reduce the tensile RS occurring in the bulge areas.

As part of the optimizing strategy, finally a punch configuration designated as 26 × 0.5 was designed as shown in Figure 10(b). This punch configuration had 26 embossing lines with radii of 0.5 mm (Table 3). Thus, the distances between the individual embossing lines were reduced from 2 mm to 0.6 mm. Furthermore, the punch configuration 26 × 0.5 allowed a maximum embossing depth of 0.1 mm.

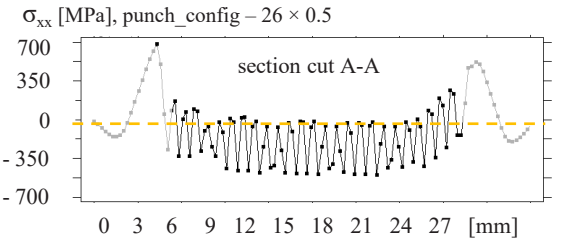

Figure 11: Residual stresses σ_{xx} of sheet metal bending specimen after embossing along section cut A-A (topside).

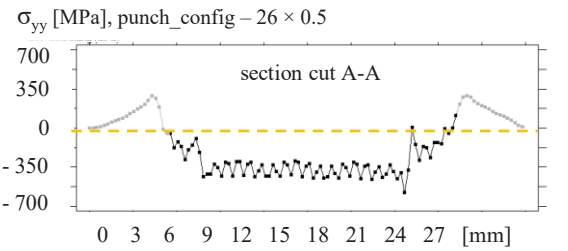

Figure 12: Residual stresses σ_{yy} of sheet metal specimen after embossing along section cut A-A (topside).

Figures 10(a) and 11 show the RS distribution σ_{xx} calculated with the punch configuration 26 × 0.5 after the first forming operation, which includes embossing and forming of the sheet angle specimen. Figure 11 further shows that the RS distribution is considerably more homogeneous compared to the RS distribution obtained with punch configuration 14 × 2.0 (Figure 9) from the first approach and tensile RS within the embossed area is nearly eliminated. Thus, by changing the punch geometries as described above, dominant compressive RS could be induced into the embossed area of the sheet angle specimen. Similar to the previously investigated punch geometry, the highest compressive RS values (approx. –480 MPa) occur in the embossed dimple areas. As in the previous investigations, there are unembossed areas between these dimples in which the sheet metal still retained its initial sheet thickness of 1.5 mm. In these differently produced areas, however, the compressive RS are now in the range from 0 MPa up to about 50 MPa.

In contrast to the periodic symmetrical RS distribution of high magnitude in σ_{xx}-direction (Figure 11), the RS distribution in σ_{yy}-direction shows a comparatively homogeneous distribution subsequent to the embossing process (Figure 12).

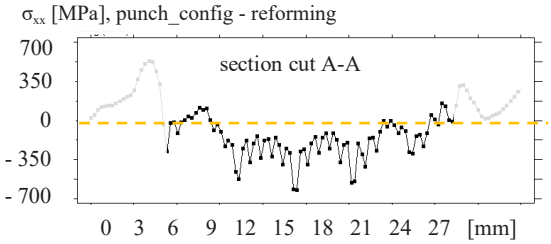

Figure 13: Residual stresses σ_{xx} of sheet metal specimen after reforming along section cut A-A (topside).

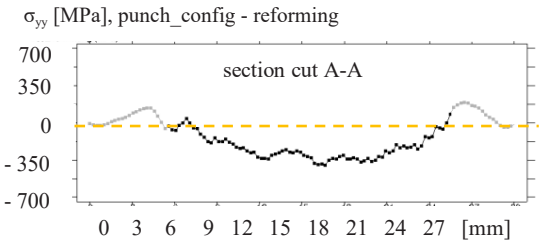

Figure 14: Residual stresses σ_{yy} of sheet metal specimen after reforming along section cut A-A (topside).

4.4 *Residual stress distribution after reforming*

The simulation results shown in Figure 13 indicate that, in contrast to the very periodic and symmetrical RS distribution in σ_{xx}-direction obtained after single embossing (Figure 11), a rather asymmetrical surface RS gradient is formed along section cut A-A by the subsequent reforming process (Figure 13). Here, the maximum compressive RS values decreases from approx. –560 MPa to about –450 MPa, while the minimum compressive RS remain at about 80 MPa. In general, it can be seen that a more homogenous RS distribution can be achieved for the stress component σ_{xx} by the sequential embossing and reforming method than by the single embossing operation. Thus, the periodic sinusoid with a delta of up to 480MPa between upper and lower peaks can be significantly reduced by the reforming operation. Regarding this stress delta, e.g. at the specimen width of 13 mm, the upper RS value of 100 MPa, and the lower RS value of approx. 220 MPa are only about 120 MPa apart.

A comparable result was obtained for the RS component σ_{yy} (Figure 14). Here, the highest values of compressive RS in y-direction remain nearly unchanged at about 350 MPa in the middle of the section cut A - A.

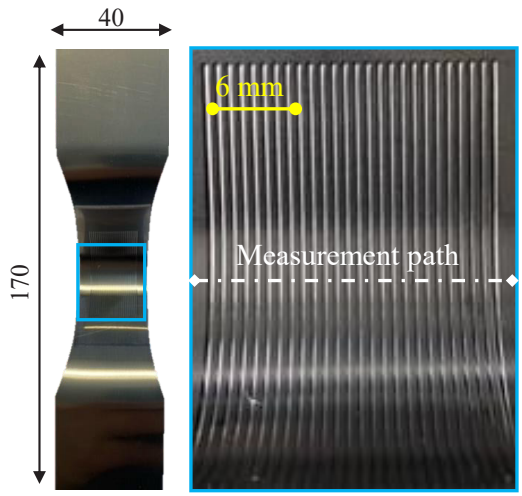

Figure 15: manufactured sheet angle bending specimen by embossing and reforming with the punch configuration 26 × 0.5 (Table 3)

In contrast, the minimum compressive RS values predominantly decrease to nearly 0 MPa. Consequently, the reforming operation leads to a more homogeneous RS distribution and lower mean compressive RS compared to the single embossing operation. Outside the embossed and reformed areas, however, balancing tensile RS occurs. Since such concentrated tensile RS can impair the fatigue strength of the embossed sheet metal components, current research work is concerned with relocating these RS to non-critical component areas. This can be done by using an appropriate design of the embossing punch. However, the final design strongly depend on the components geometry and its complexity.

5 Experimental Method

The experimental investigations on sequential embossing and reforming were carried out using a conventional hydraulic press "Metallkraft WPP 60 MVZ" and a specifically manufactured embossing and reforming tool with the described punch configuration 26 × 0.5 (Table 3) in dry condition, i.e. without lubricant. The sheet metal specimens used were cut from the stainless steel blanks and had a size of 220 × 40 × 1.5 mm. The punch force was set to $P_f = 600$ kN for embossing and approx. 400 kN for reforming. Figure 15 shows one of the embossed and reformed specimen produced.

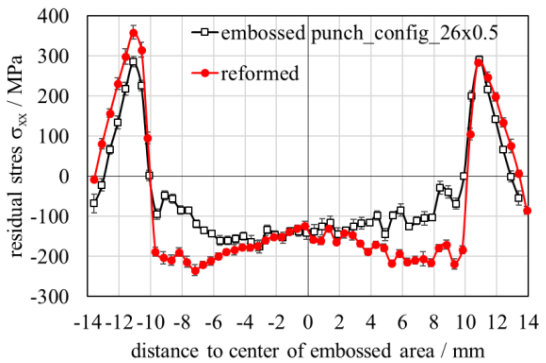

Figure 16: Residual stress distribution σ_{xx} determined using XRD on the embossed and the embossed + reformed sheet angle bending specimen (inside radius).

The near-surface RS distributions of the specimens produced were determined by means of X-ray diffraction (XRD) according to the $\sin^2\psi$-method [10]. For this purpose, a conventional ψ-diffractometer and V-filtered Cr-Kα radiation were used to analyze the {211}-ferrite diffraction line ($2\theta_0$ = 155.35°). The beam was collimated, using a 1 mm round collimator on the primary side and a 4 mm symmetrization slit in front of the scintillation counter [11]. The RS component in tangential direction σ_{xx} was analyzed for 54 measuring points across the embossed and reformed area (measurement path) at the inside radius, as shown in Figure 15. For each measuring point, 15 tilt angles ψ in a range between $-45° \leq \psi \leq 45°$ were applied, equidistantly distributed in $\sin^2\psi$. The stress evaluation was performed using the lattice specific diffraction elastic constants (DEC) $E^{\{211\}}$ = 219911 MPa and $\nu^{\{211\}}$ = 0.28, calculated from single-crystal elastic constants according to [12].

Figure 16 depicts the experimentally determined RS distribution along the measurement path illustrated in Figure 15 for the embossed state (blue marks) and the additionally reformed state (orange marks) of one of the formed test specimens. It can be observed that compressive RS were obtained across the complete embossed area. The lateral distribution of the compressive RS shows a maximum of approx. –150 MPa at the centre of the embossed area and slightly decreasing compressive RS towards the two edges of the embossed field. After the subsequent reforming process, the compressive RS show a significant increase in magnitude towards the two edges of the embossed area up to about –250 MPa. The compressive RS located in the center of the embossed field as well as the compensating tensile RS with peaks of up to about 350 MPa on the left and right-hand side of the deformed area remain nearly unchanged after the reforming process. Due to the comparable large size of the XRD measuring spot of approx. 1.5 mm, the sinusoidal RS distribution across the deformed area, which was predicted by the numerical simulation, could not be validated experimentally. However, the calculated compressive and tensile RS distribution after embossing and reforming are qualitatively confirmed by the experimental investigation.

6 Conclusions

A novel forming strategy based on a sequential one-sided embossing and reforming process was proposed, which allows for the local generation of residual stresses during a sheet metal forming process. The application was shown for the stainless steel sheet material (X6Cr17) with a thickness of 1.5 mm. An embossing punch having an individual number of parallel embossing line structures of 0.1 mm height was used to bend and emboss a flat sheet metal blank into a sheet angle specimen. In a second operation, a flat punch was used to reform the previously embossed area in order to flatten the stress curves.

From the numerical and experimental studies the following conclusions can be drawn:

- It has been found, that sequential embossing and reforming is a suitable method for the tailored induction of compressive residual stresses into sheet metal blanks.
- A significant advantage of the novel approach is the integration of the embossing and reforming process into conventional sheet metal forming as e.g. deep drawing and crash forming. This way further mechanical post-process surface treatment can be omitted.
- By the first process step of our forming strategy, i.e. the embossing step, a characteristic periodically alternating residual stress distribution is generated, which exhibits compressive RS in the dimples and tensile RS in the bulge regions.
- By means of the second process step, i.e. the reforming, only the bulge regions were plastically deformed. The reforming operation led to a reduction

in amplitude of the periodic residual stress distribution and hence contributes to its homogenization.

- Experimental residual stress analysis on sheet metal angle specimen that were processed using the novel forming strategy confirmed the qualitative course of the numerical results, but also revealed that the simulation obviously overestimates the compressive residual stress values.

Acknowledgments

This research was funded by the German Research Foundation (DFG) in the DFG priority program "SPP2013 Targeted use of forming induced residual stresses in metal components" (Gi 376/13-2, Bo 1466/14-2, Li 1556/61-2). The support by the German Research Foundation (DFG) is gratefully acknowledged The results of this work are based upon numerical investigations and experiments performed at the Institute for Forming Technology (IFU) of University of Stuttgart, IAM-WK and ITM of Karlsruhe Institute for Technology (KIT), Germany.

References

[1] M. Liewald and A. Weiß, "Szenarische volumenbetrachtung von kaltmassivprodukten zwischen verbrenner und elektromobilität," presented at the Umformtechnisches Kolloqium Darmstadt, Hessen, Germany, Sep. 2018.

[2] H. Behnken and V. Hauk, "On the influence of microresidual stresses during cyclic loading," in *Residual Stresses*. Germany: Oberursel, 1993, pp. 733 – 742.

[3] E. R. de los Rios, A. Walley, M. Milan, and G. Hammersley, "Fatigue crack initiation and propagation on shot-peened surfaces in A316 stainless steel," *International Journal of Fatigue*, vol. 17, no. 7, pp. 493–499, 1995.

[4] H. E. Friedrich, *Leichtbau in der Fahrzeugtechnik.* Hessen, Germany: Springer Fachmedien, 2013

[5] M. Liewald, R. Schleich, D. Vlahovic, and M. Sindel, "Einfluss dehnungsabhängiger werkstoffeigenschaften auf die umformbarkeit von blechwerkstoffen," in *Materialwissenschaft und Werkstofftechnik*. Weinheim, Germany: Wiley-VCH-Verlag, 2007.

[6] Toyota, "Toyota Motor Corporation," 2021. [Online]. Available: https://global.toyota/en/

[7] E. Kröner, "Berechnung der elastischen konstanten des vielkristalls aus den konstanten des einkristalls," *Zeitschrift für Physik*, vol. 151, no. 4, p. 504, 1958.

[8] R. Hill, "A theory of the yielding and plastic flow of anisotropic metals," *Proceedings of the Royal Society A: Mathematical, Physical and Engineering Sciences*, vol. 193, no. 1033, p. 281, 1948.

[9] E. Doege and B.-A. Behrens, "Gründliche und kompakte darstellung der umformtechnik," in *Handbuch Umformtechnik*. Berlin, Germany: Springer, 2016.

[10] E. Macherauch and P. Müller, "Das $\sin^2\psi$-Verfahren der röntgenographischen spannungsmessung," *Zeitschrift für angewandte Mathematik und Physik*, vol. 13, pp. 305–312, 1961.

[11] U. Wolfstieg, "Die Symmetrisierung unsymmetrischer interferenzlinien mit hilfe von spezialblenden," *Haerterei-Technische Mitteilungen*, vol. 31, pp. 23–26, 1976.

[12] V. Hauk and H.-J. Nikolin, "The evaluation of the distribution of residual stresses of the I. kind (RS I) and of the II. kind (RS II) in textured materials," *Textures and Microstructures*, vol. 8–9, pp. 693–716, 1988.